

Substrate Atomic-Termination-Induced Anisotropic Growth of ZnO Nanowires/Nanorods by the VLS Process

Pu Xian Gao[†] and Zhong L. Wang^{*,†,‡}

School of Materials Science and Engineering and School of Chemistry and Biochemistry,
Georgia Institute of Technology, Atlanta, Georgia 30332-0245

Received: January 23, 2004; In Final Form: March 4, 2004

In the vapor–liquid–solid (VLS) growth of 1D nanostructures, the electronic structure of the substrate surface may critically affect the morphology of the grown nanowires/nanorods. In this paper, using a model system of the Sn-catalyzed growth of ZnO nanostructures on a single-crystal ZnO substrate, we demonstrate the effect of substrate surface termination on nanowire growth. Symmetric nanoribbons have been grown on the nonpolar surfaces of $\pm(2\bar{1}\bar{1}0)$ (or $\pm(01\bar{1}0)$), but the polar surface $\pm(0001)$ substrates have asymmetrically grown nanostructures. For the Zn-terminated (0001) substrate surface, uniform, long, and epitaxially aligned nanowires have been grown. For the oxygen-terminated (000 $\bar{1}$) substrate surface, short nanotrunks have been grown. These asymmetrical growth features are related to the atomic termination of the substrate, surface charges, and interface adhesion. These observations provide some insight into the physical chemical process in VLS growth.

Wurtzite ZnO has two important structural characteristics: noncentral symmetry and polar surfaces. Zn²⁺ and O²⁻ are tetragonally coordinated so that the center of the positive charges overlaps with that of the negative charges. If subjected to an external force, the distortion of the tetrahedron results in a dipole moment, leading to the piezoelectric effect.¹ From the structural point of view, Zn and oxygen atoms are arranged alternatively layer-by-layer along the *c* axis so that the top surface is Zn²⁺-terminated (0001) and the bottom surface is O²⁻-terminated (000 $\bar{1}$). The opposite ionic charges on the surfaces result in a spontaneous polarization. The polar surfaces of ZnO are very stable and have not been reconstructed,² and they have been used to induce the formation of some novel nanostructures such as nanohelicals (nanosprings),³ nanorings,⁴ and nanobows.⁵ Recently, the Zn-terminated (0001) surface has been shown to be effective for growing nanostructures, but the oxygen-terminated (000 $\bar{1}$) surface is chemically inert, resulting in the growth of a “comb”-like structure in the vapor–solid process without using a catalyst.⁶ The growth was suggested to be a self-catalysis process due to Zn-termination at the (0001) surface.

In vapor–liquid–solid (VLS) growth,⁷ it is generally believed that it is the catalyst particle at the tip that determines the size and growth rate of the nanowire, and the surface termination of the substrate may have little effect on the growth. Controlling the size of the catalyst particles can effectively control the size of semiconductor nanowires.⁸ In this paper, taking the Sn-catalyzed growth of 1D nanostructures of ZnO on a single-crystal ZnO substrate as a model system, we show that the substrate atomic termination can critically affect the growth rate and morphology of the grown nanowires in VLS growth. The growth features on the $\{2\bar{1}\bar{1}0\}$, $\{01\bar{1}0\}$, and $\pm(0001)$ surfaces will be elaborated. It is suggested that the interaction between

the surface ionic charge with the catalyst particle is likely responsible for the observed growth phenomena.

The sample used in this study was prepared using a two-step high-temperature vapor–solid deposition process, which was used for growing the polar-surface-dominated nanopropeller arrays of ZnO.⁹ The solid vapor deposition here involves using an experimental setup consisting of a horizontal high-temperature tube furnace (~ 50 cm in length), an alumina tube (~ 75 cm in length, ~ 4 cm in inner diameter), a rotary pump system, and a gas controlling system. Commercial (Alfa Aesar) ZnO and SnO₂ powders and graphite with a molar ratio of 3:4:1.5 were mixed, ground, and then loaded onto an alumina boat and positioned at the center of the alumina tube. The evaporation was conducted at 1100 °C for 60 min (step I) and then up to 1300 °C for half an hour (step II) under a pressure of 200 mbar. The N₂ carrier gas flow rate is controlled at 20 sccm. The desired structures grew on a polycrystalline Al₂O₃ substrate in temperature zones ranging from 600 to 700 °C and 800 to 900 °C, respectively, corresponding to lower- and higher-temperature duration periods.

The as-grown sample has many large crystals of ZnO formed on the alumina substrate, and these ZnO crystals serve as the substrate for growing ZnO nanostructures. Figure 1a shows a typical scanning electron microscopy (SEM) image of a large block of the as-grown ZnO nanostructures, which looks like a “brush” that is 40–50 μm in length, 10–15 μm in width, and several micrometers in thickness. A large ZnO crystal is the substrate with aligned ZnO nanostructures growing out of the five exposed surfaces and displaying different growth features. Energy-dispersive spectroscopy (EDS) analysis in SEM proves that the as-grown base and the as-grown nanostructures are ZnO with Sn balls at the tips. The nanostructures grown at the left- and right-hand-side facets are distributed symmetrically, but the top and bottom surfaces have asymmetrical nanostructures of different dimensionality and morphology. On the top facet, the grown elements are short, conelike trunks ~ 1 μm in height and 800 nm in width. On the bottom surfaces, uniform nanowires

* Corresponding author. E-mail: zhong.wang@mse.gatech.edu.

[†] School of Materials Science and Engineering.

[‡] School of Chemistry and Biochemistry.

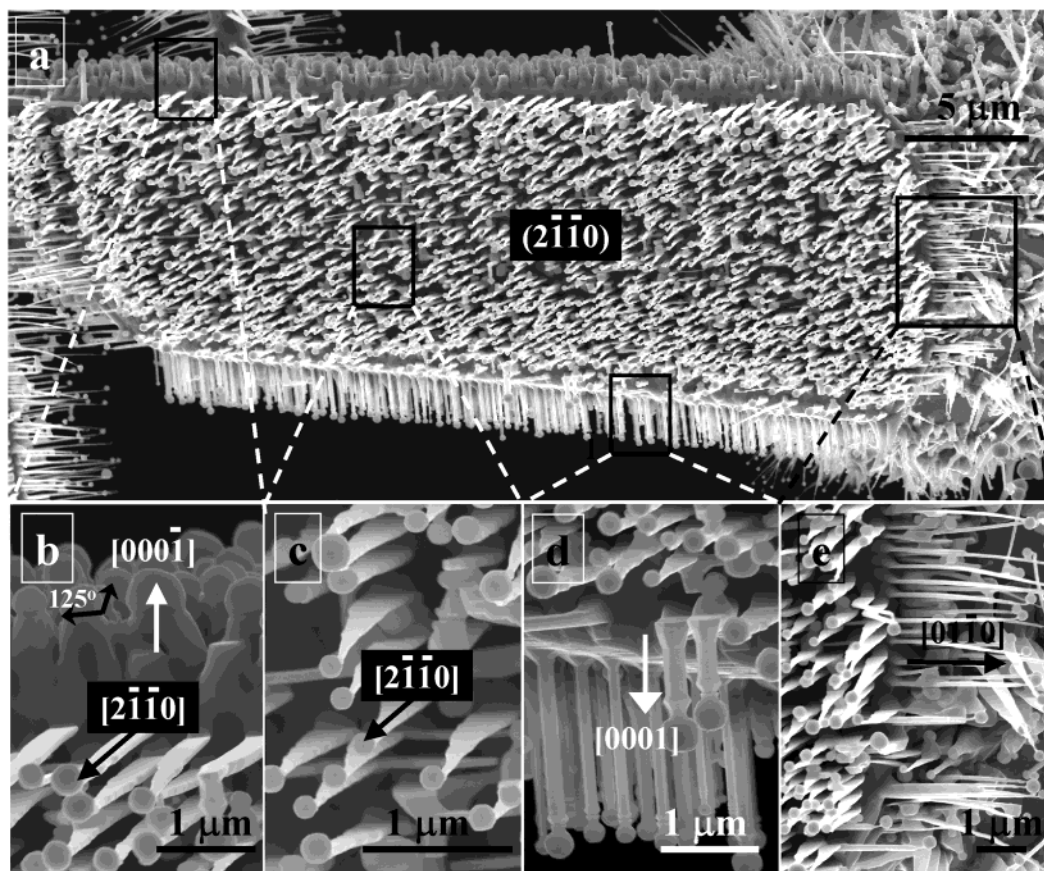


Figure 1. SEM images of the as-synthesized ZnO nanostructures growing out of the five surfaces of a ZnO substrate. (b–e) Enlarged areas as marked in a. The asymmetric growth of nanostructures on the substrate surfaces of different structure characteristics is presented. (See the text.)

with a diameter of ~ 100 nm and a height of ~ 2 μm are grown. On the basis of our recent study on ZnO nanopropellers, the Zn-terminated (0001) planes are active for nanowire growth, but the oxygen-terminated (000 $\bar{1}$) plane is inert with Sn-guided growth;⁹ the top and bottom surfaces in Figure 1a are (0001) and +(0001), respectively.

For the nanotrunk growth on the (000 $\bar{1}$) surface, the contact angle between the Sn ball and the trunk top is $\sim 125 \pm 5^\circ$ (Figure 1b). Figure 1d is the magnified side view of the as-grown nanowires on the Zn-terminated (0001) surface. The aligned ZnO nanowires grown out of the Zn-terminated (0001) surface have a uniform diameter of ~ 100 nm and a length of ~ 2 μm and six side surfaces $\{2\bar{1}\bar{1}0\}$ (Figure 1d).^{10,11} The nanowires are aligned, and they have an epitaxial orientation with respect to the substrate. The contact angle between the Sn particle and the nanowire growth front is $\sim 150 \pm 5^\circ$.

Figure 1c shows the well-aligned ZnO nanoribbons growing out of the $(2\bar{1}\bar{1}0)$ surface of the substrate, with epitaxial growth direction $[2\bar{1}\bar{1}0]$, top and bottom faces $\pm(0001)$, and side-stepped $(01\bar{1}0)$ surfaces. The width of the nanoribbon is not uniform along the entire length. The nanoribbon has the largest width of ~ 300 nm at the contact point with the substrate, the smallest width of ~ 10 nm at the contact with the Sn catalyst, and a length of ~ 1 μm . Figure 1e shows the normally orientated nanoribbons on the right-hand-side facet of the substrate, which grow along $[01\bar{1}0]$. It is also shown that the widths of the nanoribbons along $[2\bar{1}\bar{1}0]$ and $[01\bar{1}0]$ are of the same order of magnitude, tens of nanometers, and that the length of the nanoribbons along $[01\bar{1}0]$ is around 3 μm .

The nonpolar surface shows symmetric growth. Figure 2 is a top view along the c axis of the nanowires grown on a ZnO

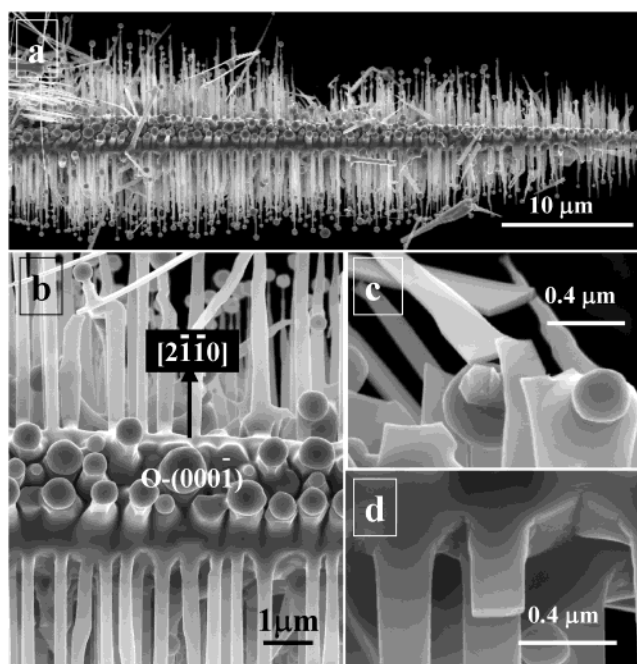


Figure 2. (a) [0001] directional top view of the as-grown ZnO nanostructures, showing the symmetric growth of triangular nanoribbons along $\pm[2\bar{1}\bar{1}0]$. (b) Closer top view of the nanotrunk growth out of the O-terminated (000 $\bar{1}$) ZnO surface, revealing the hexagonal base contour of nanopyramids. (c) Broken triangular nanoribbons showing rectangular cross sections. (d) Smooth top surfaces of triangular nanoribbons corresponding to the O-terminated (000 $\bar{1}$) polar surface of ZnO.

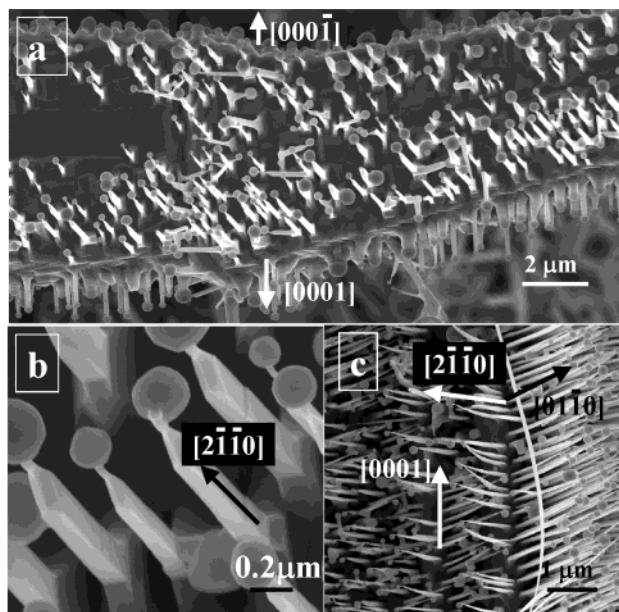


Figure 3. (a) As-grown ZnO nanostructures with a $(2\bar{1}\bar{1}0)$ plane that is sparsely covered by ZnO nanoribbons. (b) Closer view of the nanoribbons normal to the $(2\bar{1}\bar{1}0)$ plane, indicating nanoribbons with small width/thickness ratio. (c) Periodically aligned arrays of ZnO nanoribbons with growth directions of $[2\bar{1}\bar{1}0]$ and $[0\bar{1}\bar{1}0]$ on the two surfaces, respectively.

substrate. It is apparent that the triangular nanoribbons are grown symmetrically on the top and bottom nonpolar facets of $\pm(2\bar{1}\bar{1}0)$. From Figure 2b, it was found that the cone trunks that formed vertically on the O-terminated $(000\bar{1})$ top surface have roughly faceted side surfaces, defined by $\{2\bar{1}\bar{1}0\}$ and displaying a hexagon-based pyramid. In Figure 2c, the broken triangular nanoribbons clearly present their rectangular cross section of ~ 300 nm in width and ~ 40 nm in thickness. A closer image at the top surface of the nanoribbon displays a smooth top surface (Figure 2d), corresponding to the chemically sluggish O-terminated $(000\bar{1})$ polar surface of ZnO, consistent with our previous results.⁶

Figure 3a shows another SEM view from the top of the brush structure. On the top and bottom O- $(000\bar{1})$ and Zn- (0001) ZnO surfaces, aligned shorter and wider pyramidal ZnO trunks and longer and narrower hexagonal ZnO nanowires are grown, respectively. Different from the cases in Figures 1 and 2, the nanoribbons grown on the large $(2\bar{1}\bar{1}0)$ substrate surface could have a smaller width-to-thickness ratio. The grown nanoribbons are enclosed by relatively larger and smoother $\pm(01\bar{1}0)$ surfaces and smaller $\pm(0001)$ surfaces. Steps are introduced on the side surfaces, and the nanoribbon becomes sharper toward the tip (Figure 3b). The interval between the nanoribbons is quite regular, and the aligned ribbon spacing is close to periodic (Figure 3c).

On the basis of the SEM image in Figure 1, we have calculated the volumes of the as-grown ZnO nanostructures and the Sn particles covering the unit substrate surface area of the $\pm(0001)$ polar surfaces. We assume that the nanostructures on both polar surfaces are uniformly distributed, and the Sn particles are spherical, the ZnO nanowires are cylindrical, and the ZnO pyramidal trunks have a hexagon base. The estimated volumes of ZnO nanostructures and Sn catalysts per unit area are 197 ± 5 (ZnO nanowires) and 600 ± 10 nm (Sn catalysts) for the (0001) substrate surface and 318 ± 9 (ZnO pyramidal trunks) and 854 ± 20 nm (catalyst Sn) for the $(000\bar{1})$ substrate surface, respectively. The volume ratio of the ZnO material per unit area

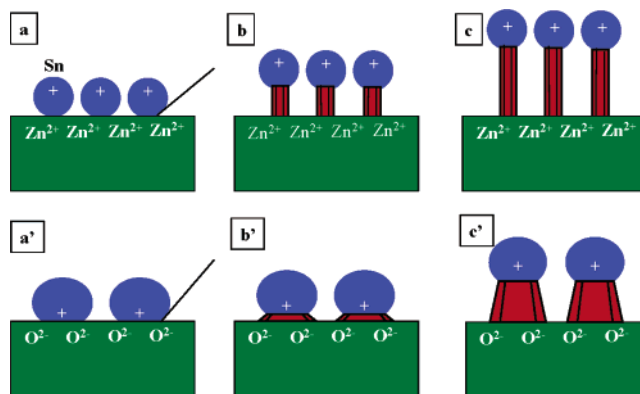
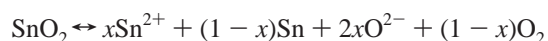


Figure 4. Growth model of the ZnO nanowires on a Zn-terminated (0001) polar surface (a–c) and an O-terminated $(000\bar{1})$ polar surface (a'–c'). (See the text.)

on the (0001) and $(000\bar{1})$ substrate surfaces is 1:1.6, and the volume ratio of the Sn material per unit area on the (0001) and $(000\bar{1})$ substrate surfaces is 1:1.42. The volume ratios of ZnO/Sn on the (0001) and $(000\bar{1})$ substrate surfaces are 3 and 2.7, respectively, indicating that the sticking rates of the ZnO vapor onto the Sn surfaces are not significantly different on the two substrate surfaces, but the amounts of ZnO and Sn deposited on the $(000\bar{1})$ substrate surface are about 50% more than that deposited onto the (0001) substrate surface, indicating the high surface adsorption rate of Sn onto the $(000\bar{1})$ substrate surface.

From Figure 1b and d, the contacting angle between the Sn particle and the ZnO nanowire is $\sim 150^\circ$ on the Zn-terminated (0001) substrate surface and $\sim 125^\circ$ on the oxygen-terminated $(000\bar{1})$ substrate surface, indicating that the $(000\bar{1})$ surface has a higher degree of wetting contact with the Sn particle than the (0001) surface.

On the basis of the experimental data presented, a growth model for the ZnO nanostructure growth on $\pm(0001)$ polar surfaces is proposed. The entire growth is dominated by VLS. The Sn catalyst was reduced from SnO_2 added to the source material.¹² The thermal reduction of SnO_2 may result in some charged species and neutral:



where x represents the percentage of charged Sn^{2+} ions after the decomposition. The charged species may recombine and condense onto the substrate to form a charged catalyst particle $(\text{Sn})^+$. A neutral Sn particle can also be positively charged because metal atoms tend to lose electrons.¹³ For the Zn^{2+} -terminated (0001) ZnO substrate surface with positive charges, the positively charged $(\text{Sn})^+$ particle has a small repulsion with the substrate because of the electrostatic interaction, but it still tends to stick onto the surface because of a stronger adhesion force. The consequence of the electrostatic repulsion results in a larger contact angle between the particle and the substrate (Figure 4a). The Sn particle initiates the growth of the ZnO nanowire (Figure 4b), and the nanowire has an epitaxial orientation relationship with the substrate because of least lattice mismatch.¹⁰ The nanowire continues to grow following the VLS growth process (Figure 4c).

For the oxygen-terminated $(000\bar{1})$ ZnO substrate surface with negative charges, the attraction between the substrate surface and the positively charged $(\text{Sn})^+$ particle results in a smaller contact angle and a larger contact area (Figure 4a'). Naturally, there is a lower population density of Sn particles on the substrate surface, and each of them is larger. The large Sn

particle initiates the growth of nanorods (Figure 4b'). As the growth continues and the distance between the particle and the substrate surface is further away, the contact area between the particle and the ZnO nanorod may decrease slightly because of the reduced electrostatic attraction, possibly resulting in a shrinkage in nanorod size as the growth proceeds and forming a short nanotrunk with a hexagon base (Figure 4c').

In comparison to the growth on the (0001) substrate surface, the electrostatic attraction between the (000 $\bar{1}$) substrate surface and the Sn particles tends to attract a high density of Sn onto the surface in early growth stages. These Sn particles are most effective in attracting the ZnO molecular species, resulting in a higher density of ZnO deposition onto the (000 $\bar{1}$) substrate surface. But the ratio of ZnO/Sn in each case remains approximately a constant, as expected from the VLS process in which it is the catalyst surface that is responsible for adsorbing the incoming molecular species.

For the nonpolar $\pm(2\bar{1}\bar{1}0)$ and $\pm(01\bar{1}0)$ substrate surfaces, the growth on the surfaces shows symmetric features and still follows the VLS growth process. Take the $(2\bar{1}\bar{1}0)$ substrate surface as an example. Nanoribbons grow epitaxially on the substrate; they are enclosed by large $\pm(01\bar{1}0)$ and small $\pm(0001)$ surfaces, and gradual lateral growth along $\pm[01\bar{1}0]$ results in a triangular-like shape. (See Figure 1c.)

In summary, Sn-catalyzed ZnO nanostructure growth on a single-crystal ZnO substrate has been used as a model system for elaborating the effect of polar surfaces on the VLS growth of nanowires. For the Zn-terminated (0001) substrate surface, because of an electrostatic repulsion between the Sn particle and the substrate, uniform, long, and epitaxially aligned nanowires have been grown. For the O-terminated (000 $\bar{1}$) substrate surface, short nanotrunks have been grown; these are attributed

to a stronger adhesion between the substrate and the particle in the initial stage of growth. These asymmetric growth features are related to the atomic termination of the substrate, surface charges, and interface adhesion, but the volume ratio of ZnO/Sn on the two polar surfaces remains about the same, indicating that the VLS process is dominant. For nonpolar surfaces such as $\pm(2\bar{1}\bar{1}0)$ (or $\pm(01\bar{1}0)$), symmetric nanoribbons have been grown. The growth model proposed here might provide some new insight in understanding the physical chemical process involved in VLS growth.

Acknowledgment. We are grateful for financial support from the NASA Vehicle Systems Program and Department of Defense Research and Engineering (DDR&E). We thank Dr. Zhenyu Zhang for stimulating discussions.

References and Notes

- (1) Wang, Z. L.; Kang, Z. C. *Functional and Smart Materials: Structure Evolution and Structure Analysis*; Plenum Press: New York, 1998; Chapter 1.
- (2) Meyer, B.; Marx, D. *Phys. Rev. B* **2003**, *67*, 035403.
- (3) Kong, X. Y.; Wang, Z. L. *Nano Lett.* **2003**, *3*, 1625.
- (4) Kong, X. Y.; Ding, Y.; Yang, R. S.; Wang, Z. L. *Science* **2004**, *303*, 1348.
- (5) Hughes, W.; Wang, Z. L. *J. Am. Chem. Soc.*, in press.
- (6) Wang, Z. L.; Kong, X. Y.; Zuo, J. M. *Phys. Rev. Lett.* **2003**, *91*, 185502.
- (7) Wagner, R. S.; Ellis, W. C. *Appl. Phys. Lett.* **1964**, *4*, 89.
- (8) Morales, A. M.; Lieber, C. M. *Science* **1998**, *279*, 208.
- (9) Gao, P. X.; Wang, Z. L. *Appl. Phys. Lett.* **2004**, *84*, 2883.
- (10) Gao, P. X.; Ding, Y.; Wang, Z. L. *Nano Lett.* **2003**, *3*, 1315.
- (11) Ding, Y.; Gao, P. X.; Wang, Z. L. *J. Am. Chem. Soc.* **2004**, *126*, 2066.
- (12) Gao, P. X.; Wang, Z. L. *J. Phys. Chem. B* **2002**, *106*, 12653.
- (13) Parish, R. V. *The Metallic Elements*; Longman Inc.: New York, 1977.